

Effect of titanium carbide coating on the osseointegration response in vitro and in vivo

Marina Brama^a, Nicholas Rhodes^{e,*}, John Hunt^e, Andrea Ricci^a, Roberto Teghil^d, Silvia Migliaccio^b, Carlo Della Rocca^c, Silvia Leccisotti^a, Attilio Lioi^a, Marta Scandurra^a, Giovanni De Maria^f, Daniela Ferro^f, Fanrong Pu^e, Gianluca Panzini^g, Laura Politi^a, Roberto Scandurra^a

^aDipartimento di Scienze Biochimiche, Università 'La Sapienza', Ple A. Moro, 5, 00185 Roma, Italy

^bDipartimento di Fisiopatologia Medica, Università 'La Sapienza', Viale del Policlinico 155, 00161 Roma, Italy

^cDipartimento di Medicina Sperimentale e Patologia, Università 'La Sapienza', Viale Regina Elena 324, 00161 Roma, Italy

^dDipartimento di Chimica, Università della Basilicata, N. Sauro 85, 85100 Potenza, Italy

^eUK Centre for Tissue Engineering, Department of Clinical Engineering, Daulby Street, Liverpool L69 3GA, UK

^fDipartimento di Chimica, Università 'La Sapienza', Ple A. Moro, 5, 00185 Roma, Italy

^gServizio Biologico e per la gestione della Sperimentazione Animale, Istituto Superiore di Sanità, Viale Regina Elena 299, 00161 Roma, Italy

Received 11 May 2006; accepted 11 August 2006

Abstract

Titanium has limitations in its clinical performance in dental and orthopaedic applications. This study describes a coating process using pulsed laser deposition (PLD) technology to produce surfaces of titanium carbide (TiC) on titanium substrates and evaluates the biological response both in vitro and in vivo. X-ray photoelectron spectroscopy (XPS) analysis revealed the presence of 18.6–21.5% TiC in the surface layer, accompanied by oxides of titanium 78.5–81.4% in the following concentrations: 11.1–13.0% Ti₂O₃, 50.8–55.8% TiO₂, 14.5–14.7% TiO. Expression of genes central to osteoblast differentiation (alkaline phosphatase, A2 pro-collagen type 1, osteocalcin, BMP-4, TGFβ and Cbfa-1) were up-regulated in all cell lines (primary human osteoblasts, hFOB1.19 and ROS.MER#14) grown on TiC compared with uncoated titanium when measured by semiquantitative PCR and real time-PCR, whilst genes involved in modulation of osteoclastogenesis and osteoclast activity (IL-6 and M-CSF) were unchanged. Bone density was shown to be greater around TiC-coated implants after 2 and 4 weeks in sheep and both 4 and 8 weeks in rabbits compared to uncoated titanium. Rapid bone deposition was demonstrated after only 2 weeks in the rabbit model when visualized with intravital staining. It is concluded that coating with TiC will, in comparison to uncoated titanium, improve implant hardness, biocompatibility through surface stability and osseointegration through improved bone growth.

© 2006 Elsevier Ltd. All rights reserved.

Keywords: Titanium; Titanium carbide; Pulsed laser deposition; Plasma coating; Osseointegration

1. Introduction

The biocompatibility of orthopaedic or dental implants depends largely on the effect of the implant on bone-forming cells, namely osteoblasts. A stable connection between the biomaterial surface and the surrounding tissue is one of the most important prerequisites for the long-term

success of such implants. Hence, a strong integration of the tissue with the implant surface is required. Titanium is the most widely used material in dental and orthopaedic implants due to its superior physical properties such as low specific gravity, low elastic modulus and enhanced biocompatibility that is reported in comparison to other, often less expensive, metals and alloys.

However, in spite of these characteristics and its clinical prevalence, titanium suffers from a reduction in its bone integrative properties after sustained exposure to

*Corresponding author. Tel.: +44 151 7064211; fax: +44 151 7064915.
E-mail address: npr@liv.ac.uk (N. Rhodes).

a physiological environment. The problem has been outlined in a recent review [1]. In particular, the nature and properties of the oxides present in the near-surface region deserve special attention. The titanium oxides from TiO to Ti₃O₅ could possibly exist in a stable state within the environmental conditions surrounding an implant [2,3]. Tribo-chemical reactions during use can modify the surface of an implant producing wear debris accumulation which results in adverse cellular responses leading to inflammation, release of harmful enzymes, bone cell lysis (osteolysis) and implant loosening [1,3,4].

Surface modification of implanted devices that prevented alteration of the oxide layer could be used to improve bone response and efficacy of the device in vivo, using either bioinert or bioactive materials. Of the former, titanium carbide (TiC) coatings could be considered a good candidate due to their ability to form strong bonds with the titanium substrate and their possession of superior hardness and wear resistance, with the potential for excellent biocompatibility due to the introduction of carbon atoms into the metal matrix. TiC coating of titanium devices should therefore produce a triple effect: protection of the metal against oxidation; significant increase in hardness improving the tribo-chemical behaviour, particularly wear resistance; and improvement in integrative performance of the implanted device improving biocompatibility.

Chemical vapour phase deposition (CVD) or physical vapour phase deposition (PVD) are commonly used to cover a metal surface with a thin layer of carbide [5], producing extremely uniform films. Another technique, pulsed laser deposition (PLD) has also been successfully utilized [6]. In this latter technique, when a solid target is irradiated by a focalized pulsed laser beam, a gaseous cloud, called plume for its shape, is produced. The plume, a plasma composed of electrons, atoms, ions, molecules, clusters and, in some cases, droplets and target fragments, expands, either in vacuum or in a gaseous environment, and will become deposited on a substrate giving rise to a film. The particles forming the plasma have a high kinetic energy (about 60 eV), much higher than in other deposition techniques [7], allowing them to interact effectively with a reactive gas, if present within the deposition chamber. They also have great mobility on the deposition substrate, avoiding the necessity for high substrate temperature. In the interaction between the target and the laser beam many different thermal and electronic mechanisms are involved [6], but in general the composition of the gaseous phase is often very different from that found in thermal equilibrium vaporization allowing the deposition of materials with a complex stoichiometry. For all these unique characteristics, PLD has been widely used in the last 10 years to deposit thin films of materials of technological interest [8,9]. It has been demonstrated that the hardness of the resultant surface depends strongly on the film thickness and PLD operating conditions for carbides of hafnium and titanium on silica substrates [10,11].

In this context, the present study was designed to characterize the microstructure, the film-substrate interface and the biological response in vitro of a range of different cell types: a rat osteosarcoma line ROS.MER#14 developed by one of us [12], a human foetal osteoblast line (hFOB 1.19) and primary human osteoblasts (hOB), because of a possible future application of a TiC coating on human prostheses. It was considered desirable to evaluate this response on different cell types to understand both the typical, but rather variable response of primary cell cultures, and the less variable but possibly less realistic response of a cell line. The cells were cultured on titanium samples coated by TiC evaluating the expression of genes central to bone turnover, indicating different aspects of the process, from proliferation (alkaline phosphatase, ALP), matrix formation (A2 pro-collagen type 1, COL1A2) and mineralization (osteocalcin, OC; bone morphogenic protein-4, BMP-4; transforming growth factor β , TGF β and Core binding factor-1/osteoblast specific factor 2, Cbfa1/osf2). We also evaluated the response of bone tissue in vivo to titanium implants coated by TiC to demonstrate that the indicative gene upregulation resulted in genuine improved bone growth.

2. Materials and methods

2.1. Titanium substrates

Titanium grade 2 (Ti = 99.85%; C = 0.0006%; Ni = 0.01%; O = 0.1%; H = 0.003%; Se = 0.03%) was used in all experiments in this study. For in vitro experiments, rods were cut into disks (13 mm diameter, 2 mm thick) that were used either rough cut, mirror polished or blasted with 60, 120 or 150 μ m zirconia particles. Dental implants (4 mm diameter \times 8 mm) obtained from Orvit (Bologna, Italy) were used for in vivo implantation in both New Zealand rabbits (performed at the Department of Animal Experimentation of Istituto Superiore di Sanità, Rome) and sheep (performed at the Department of Animal Surgery of Istituto Ortopedico Rizzoli, Bologna). Additionally, in vivo implants in the rabbit using 2 mm diameter rods, 5 mm in length were performed at the Department of Clinical Engineering of the UK Centre for Tissue Engineering, Liverpool [13]. All samples for in vivo implantation were sandblasted with 120 μ m zirconia particles.

2.2. TiC coating

The TiC coatings were deposited on titanium substrates by the use of PLD apparatus that has been described in detail elsewhere [14]. A diagrammatic representation of the experimental assembly is shown in Fig. 1. Hot pressed TiC disks (Cerac, WI, USA) were used as targets. During the deposition process the titanium substrate was kept at constant temperature (20–600 °C). Deposition was carried out in a dynamic vacuum of 1.5×10^{-4} Pa. A frequency doubled Nd:Yag laser ($\lambda = 532$ nm, $t = 10$ ns, repetition rate 10 Hz) was utilized. The laser beam was oriented with an inclination angle of 45° with respect to the target and the substrate disk was placed at a distance of 5–15 mm from the target. Laser fluence was varied in the range 5–15 J/cm². Deposition time was 1 h for all samples and the target was maintained in a rotating motion during laser irradiation to minimize the formation of craters.

Some samples of titanium were deposited with the PLD technology at a distance of 60 mm in order to obtain a flat deposition without microroughness. Samples for in vivo ovine implantation were deposited

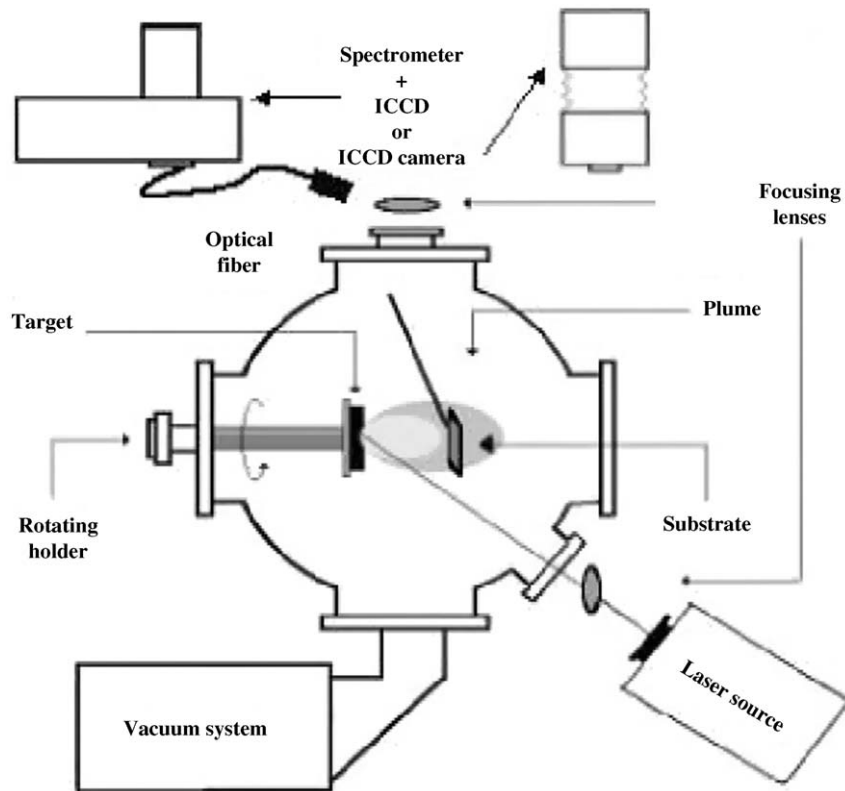


Fig. 1. Pulsed laser deposition (PLD) apparatus. When a solid target is irradiated by a focalized pulsed laser beam, a gaseous cloud, known as a plume due to its shape, is produced. The plume, a plasma composed of electrons, atoms, ions, molecules, clusters and, in some cases, droplets and target fragments, expands in vacuum and will be deposited on the substrate giving rise to a film where fragments of the target (spalls) may be inserted. The process is controlled by the spectrometer and the intensified charge coupled device (ICCD).

with a uniform coating by continuous rotation of the implant for 1 h at a distance of 8 mm from the carbide target.

Hardness of the layer obtained with PLD was tested by a Leica VMHT apparatus (Leitz, Westlar, Germany) described elsewhere [15].

Magnetron sputtering (MS) technology was also used to deposit TiC: this is an industrial PVD technique where the material is 'sputtered' from a titanium target which has its back bonded to a magnetron source and in a reactive atmosphere of ethylene (C_2H_4) and argon. An independent DC source was used to add a negative and tunable bias to the substrates during deposition. The source creates a plasma around the target, and a potential drop from the plasma to the target surface. The density of ions in the plasma is made larger by the presence of a strong magnetic field, associated with the magnetron configuration. Because of the potential drop, positive ions in the plasma—Ar ions, most often—are accelerated towards the target and collide with carbon atoms of the hydrocarbon forming TiC, which condense on the sample surface as a continuous film on the substrate placed in front of the source.

2.3. Cell culture

Three cell types were used: rat osteoblastic cells (ROS.MER#14), an osteosarcoma line of immortalized cells [12]; human foetal osteoblastic cells (hFOB 1.19) from ATCC (Rockville, MD, USA); and primary hOB isolated from bone fragments obtained from surgical procedures after obtaining full ethical consent from all donors and families.

Osteoblastic ROS.SMER#14 cells were grown as previously described [12]. Briefly, cells were cultured in a 1:1 mixture of phenol red-free Dulbecco's modified essential medium (DMEM) to F12 medium and supplemented with 5% FBS, 4 mM L-glutamine, 5 IU/ml penicillin and 5 μ g/ml streptomycin, at 37 °C in 5% CO_2 . Cells were split twice a week

and experiments were performed with cells up to passage 15. Cells were plated on experimental disks at a density of $10^6/cm^2$ and cultured for 24 h.

hFOB1.19 cells were cultured in accordance with ATCC recommendations, namely at 33.5 °C in a 1:1 mixture of DMEM:F12 supplemented with 10% charcoal-stripped FBS, 100 U/ml penicillin, 10 μ g/ml streptomycin and 300 μ g/ml geneticin in 5% CO_2 . Cells were plated on the test substrates at a density of $2 \times 10^4/cm^2$. Cells were cultured for 24 h at 39.5 °C so as to reduce cell division by inactivation of the temperature-sensitive large T antigen.

hOBs were isolated from bone fragments which were washed in sterile phosphate-buffered saline (PBS), minced, and treated with 1 mg/ml collagenase type IV and 0.25% trypsin for 30 min at 37 °C with gentle agitation. The procedure was repeated three times; cells from the second and third digestions were collected by centrifugation and plated in 25 cm^2 flasks. At confluence, the hOBs were trypsinized and amplified. They were cultured at 37 °C and maintained in DMEM supplemented with 100 μ g/ml streptomycin, 100 U/ml penicillin and 10% FBS. Test substrates were seeded with hOBs at a density of $2 \times 10^4/cm^2$ and cultured for 24 h. Cells were observed to proliferate within 4–5 days of culture, and have been shown to represent the complete phenotype of mature osteoblasts.

Proliferation within cell cultures was determined by incorporating 3H -thymidine into the cell culture medium using osteoblastic ROS.SMER#14 cells. This cell line was utilized for its reproducibility. Cells were cultured on Petri dishes (CTL), on titanium disks sandblasted with 60 μ m zirconia particles (Ti) and the latter coated with TiC were maintained in DMEM/F12 medium supplemented as described above. At 80% of confluence 1 μ Ci/ml of 3H -thymidine (Amersham International, UK; code TRK328) was added over night. The medium was discarded and the cells were rinsed four times with PBS to remove any unincorporated thymidine. Cells were lysed in 0.1% SDS for 2 h at room temperature; an aliquot was precipitated with 10% TCA (30 min at 4 °C).

The samples were centrifuged for 15 min at 3000 rpm at 4 °C. The pellets were dissolved in 0.1% SDS and the samples were transferred to scintillation vials. Radioactivity was measured in a β -counter. The results were expressed as counts/min/mg protein.

2.4. X-ray photoelectron spectroscopy (XPS) analysis

XPS analyses were performed with a Leybold LHX1 spectrometer (Leybold Vacuum, Cologne, Germany). The samples were irradiated with unmonochromatized AlK α X-rays (1486.6 eV). Survey spectra and detailed regions were recorded with a pass energy of 50 eV and channel amplitudes of 1 and 0.1 eV, respectively. Fitting efficiency was estimated by χ^2 analysis [16]. The best fit was obtained from the mass balance of the elements, taking into account stoichiometric coefficients, sensitivity factors and the accuracy limits of XPS analysis [17].

2.5. Analysis of osteoblast morphology

Osteoblastic cells (10^2) were cultured on test samples for 6 h then fixed in 2.5% glutaraldehyde in 10 mM phosphate buffer at pH 7.4 for 1 h, dehydrated in a graded ethanol series and air dried. The samples were sputter coated with gold prior to examination by scanning electron microscope using a Leo 1450VP (Carl Zeiss, Jena, Germany) running at 15 kV. Atomic force microscopy (AFM) was carried out using a Nanonics Imaging AFM (Jerusalem, Israel) in no-contact mode. A reference voltage of 0.8–1.0 V between the tip and the sample surface was used during all experiments.

2.6. RNA extraction and semiquantitative RT-PCR

Cells were washed twice with cold PBS, and total RNA was extracted using Trizol reagent (Invitrogen, Carlsbad, CA, USA). Reverse transcription was performed by adding 2 μ g total RNA and 0.5 μ g oligo (dT) to 20 μ l reaction buffer. RNA were denatured by heating to 70 °C for 10 min. First strand buffer, 2 μ l 0.1 M DTT, 1 μ l 10 μ M dNTP Mix and 1 μ l ribonuclease inhibitors (Invitrogen) was added to the reaction tube followed by incubation at 42 °C for 2 min. At the end of this reaction 200 units of Super Script II (Invitrogen) was added and incubated at 42 °C for 50 min. PCR analysis was performed using the primers described in Table 1 and with glyceraldehyde-3 phosphate-dehydrogenase (GAPDH) as an internal reference. Gene product amplification was performed in a Perkin-Elmer 2400 thermocycler, the number of cycles chosen to be in the exponential part of the PCR reaction, and using the parameters described in Table 1. Genes coding for proteins involved in bone turnover were analysed: Cbfa1/osf2, ALP, Coll-1A2, OC, BMP-4 and TGF β [18–21]; and those involved in the modulation of osteoclastogenesis and osteoclast activity: Interleukin-6 (IL-6) and macrophage colony stimulating factor (M-CSF). PCR amplified fragments were resolved by 1.0% agarose/ethidium bromide gel electrophoresis and observed under UV light.

Band areas were analysed using a Bio-Rad 670 Scanning Densitometer (Hercules, CA, USA) and Molecular Analyst software. Each value is expressed as arbitrary densitometric units normalized against values for GAPDH. Data are presented as mean \pm S.E. of at least three independent experiments. Differences were analysed by one-way analysis of variance, with $p < 0.05$ being considered statistically significant.

Table 1
Rat and human primers used in semi-quantitative RT-PCR

Target gene	Sequence	T.A. (°C)	Product size (bp)
GAPDH rat	FW 5'-CTGCACCACCAACTGCTTAG-3' RV 5'-AGATCCACAACGGATACATT-3'	54	282
GAPDH human	FW 5'-CTGCACCACCAACTGCTTAG-3' RV 5'-AGGTCCACCACTGACACGTT-3'	56	289
ALP rat	FW 5'-TGCAGTATGAGTTGAATCGG-3' RV 5'-AGGGAGGGGAGCCGGCTGTC-3'	54	704
ALP human	FW 5'-GGACATGCAGTACGAGCTGA-3' RV 5'-CACCAAATGTGAAGACGTGG-3'	55	281
COLL-1A2 rat	FW 5'-AACCTGGTCTGCTGGCTCC-3' RV 5'-ACCGGGATGGCCTTTCTCAC-3'	72	483
COLL-1A2 human	FW 5'-GTGGATACGCGGACTTTGTT-3' RV 5'-AGGTTCCACCTTCACACCAG-3'	55	600
OC rat	FW 5'-GACCCTCTCTGCTCAC-3' RV 5'-GTGGTCCGCTAGCTCGTC-3'	54	505
OC human	FW 5'-TTAAGCCAGTGCTTCACGGG-3' RV 5'-CTAGACCCGGCCGTAGAAGCG-3'	60	432
BMP-4 rat	FW 5'-AGGCGGACAGATGCTAGTT-3' RV 5'-GTCCAGGCACCATTTCTGCT-3'	58	527
BMP-4 human	FW 5'-ACCTGAGACGGGGAAGAAAA-3' RV 5'-TTAAAGAGGAAACGAAAAGCA-3'	52	354
TGF β rat	FW 5'-CTTCAGCTCCACAGAGAAGAACTGC-3' RV 5'-CACGATCATGTTGGACAACCTGCTCC-3'	72	298
TGF β human	FW 5'-CCTGCCACAGATCCCCTATT-3' RV 5'-GTGACCTCCTTGCCGTAGTAG-3'	57	509
MCS-F rat	FW 5'-GACCCTCGAGTCAACAGAGC-3' RV 5'-TTCGCGCAGTGTAGATGAAC-3'	56	382
MCS-F human	FW 5'-AGCTGCTTCACCAAGGATTAT-3' RV 5'-TCTTCTGGGACCCCAATTAGTG-3'	57	560
IL-6 rat	FW 5'-ACTTCCAGCCAGTTGCCCTTC-3' RV 5'-GGAGAGCATTGGAAGTTGGG-3'	58	389
IL-6 human	FW 5'-ATGAACTCCTTCTCCACAAG-3' RV 5'-ACATTTGCCGAAGAGCCCTCAG-3'	58	637

2.7. Real-time PCR

Quantitative reverse transcriptase-PCR (qRT-PCR) analysis was performed using an ABI Prism 7300 (Applied Biosystems, Foster City, CA, USA). Amplification was carried out with 50 ng of cDNA, in 96-well plates, using SYBR green PCR Master mix (Applied Biosystems) in 25 μ l volume. Each sample was analysed in triplicate. PCR conditions were: 94 °C for 10 min and followed by 40 cycles of 94 °C for 15 s, 60 °C for 1 min. Primers were designed using Primer Express software (Applied Biosystems) and were synthesized by Primm (Milano, Italy). The primer sequences are described in Table 2.

The results were analysed using sequence detection system (SDS) software (Applied Biosystems). Generation of double-stranded DNA was measured in real time by the increase in fluorescence caused by the spontaneous binding of SYBR green. Target gene C_t values were normalized against GAPDH (defined to be the house-keeping gene {the gene whose expression does not fluctuate}). Data were analysed using the $2^{-\Delta\Delta C_t}$ method [22,23] and expressed as fold change compared to CTL (uncoated Ti).

2.8. Implantation in sheep

Two sheep were each implanted with six TiC-coated dental implants into the left femur, with six uncoated implants inserted contralaterally into the right femur to act as controls. One sheep was sacrificed after 2 weeks, the other at 4 weeks. Implantation in sheep was carried out in accordance with Decreto Legislativo 116/92, which has been implemented in Italy in accordance with European Directive 86/609/EEC. In both animals, after anaesthesia just prior to sacrifice, an additional implant was inserted in the bone as a time zero control (panel A of Fig. 9). The implanted bones were excised, fixed in 10% formaldehyde in 0.1 M phosphate buffer, pH 7.2 and infiltrated with methacrylate resin. Each sample was dissected longitudinally and included both implant and the implant-associated tissue. Samples were processed by cutting into slices approximately 60 μ m thick using a slow speed saw and grinding. Slices were then stained with toluidine blue and acidic fucsin and observed by optical microscopy. Five non consecutive sections of each sample were observed.

2.9. Implantation in rabbits

Four New Zealand white rabbits were each implanted with one TiC-coated dental implant into their left femurs and an uncoated implant acting as a contralateral control in the right femur. After 4 and 8 weeks bone density around the implants was evaluated by an X-ray mammograph (Metaltronica, Rome, Italy) using a focal spot of 0.1 mm. After 8 weeks the animals were sacrificed and the bone containing the implant was cut using a special saw into slices of about 60 μ m and the slices exposed overnight to an X-ray low intensity microradiograph [24].

In an additional experiment, bone formation associated with each implant design was delineated through the administration of fluorescent

vital dyes at five time points after their implantation into New Zealand white rabbits following a schedule previously described [13]. Four animals were implanted with 2 mm diameter rods transcortically into their femurs, and stained by intravital fluorochromes. The flattened part of the femur was exposed by blunt muscle dissection and drill holes were made in each femur. TiC-coated implants were push fitted into the holes, with un-coated rods acting as contralateral controls, such that trans-cortical implantation was achieved. Five different intravital fluorochromes were administered intramuscularly postoperatively over a period of 8 weeks, as per the following schedule: calcein (30 mg/kg) after 1 week implantation, alizarin (25 mg/kg) after 2 weeks, oxytetracycline (25 mg/kg) after 5 weeks, xylenol orange (90 mg/kg) after 6 weeks and calcein blue (30 mg/kg) after 8 weeks. Each fluorochrome was incorporated into new bone growth during the hours following injection, therefore indicating the position of growing bone at the time of injection. One day after the final injection, the rabbits were sacrificed and their femurs removed. Each section of femur containing implants was processed into methylmethacrylate resin, sectioned with an Isomet slow speed saw, ground and polished to 50 μ m slices, then imaged using confocal microscopy.

Implantation in rabbits was performed under either UK Home Office licence or in accordance with Decreto Legislativo 116/92, which has been implemented in Italy in accordance with European Directive 86/609/EEC, as appropriate.

3. Results

3.1. Optimization of PLD process

The plot of ablation rate vs. laser fluence (Fig. 2) is not linear and can be roughly divided into the three zones I, II & III which, we believe, corresponds to different ablation mechanisms [7,25,26]. In particular, zone I corresponds to high-temperature thermal vapourization and zone II to real ablation, whilst at higher laser fluence (zone III) the laser spallation mechanism leads to an increase in the ablation rate. This hypothesis is supported by analysis of both the gaseous phase and the deposited films. In fact, it is possible to demonstrate from zone I by time of flight mass spectrometry the presence of TiC₂ in the gas phase as the main component, together with carbon and metallic titanium. This is confirmed by XPS analysis of the films deposited in this fluence range, which demonstrates the presence of carbide having TiC₂ stoichiometry, probably a metastable phase. All these data seems to indicate a high-temperature equilibrium vapourization. In fact, from equilibrium vapourization studies of carbides of

Table 2
Human primers used in real time PCR

	Primer sequences
GAPDH	5'-GGAGTCAACGGATTTGGTCGTA-3' 5'-GGCAACAATATCCACTTACCAGAGT-3'
ALP	5'-TGCGGAAGAACCCCAAAG-3' 5'-ATGGTGCCCGTGGTCAAT-3'
COLL-1A2	5'-CCCAGCCAAGAAGTGGTATAGG-3' 5'-GGCTGCCAGCATTGATAGTTTC-3'
Osteocalcin	5'-AGCAAAGGTGCAGCCTTTGT-3' 5'-GCGCCTGGGTCTCTTCACT-3'
Cbfa-1	5'-GCCAGGCAGGTGCTTCAG-3' 5'-GGATGAAATGCTTGGGAAGT-3'

transition elements, the existence of the dicarbide molecule in the gas phase is well known. At relatively low temperatures the relative quantity of this compound is very low but it increases with rising temperature up to the so-called “inversion temperature” where dicarbide becomes the main component of the equilibrium gaseous phase. For TiC, the inversion temperature has been estimated to be 5000 K, a temperature which is easily attained in the laser ablation conditions.

As laser fluence is increased, the gaseous phase shows only the presence of titanium and carbon (zone II) while

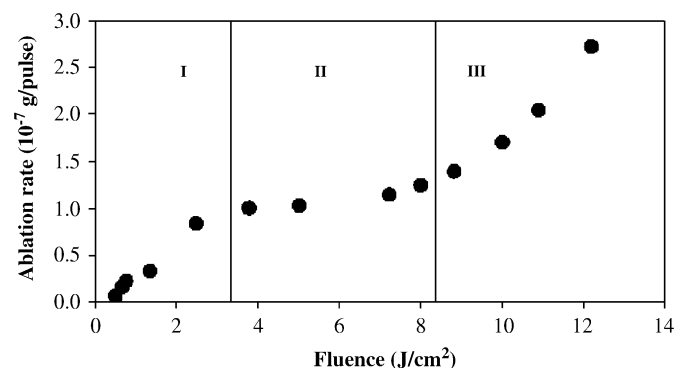


Fig. 2. Ablation rate of TiC versus the laser fluence in PLD apparatus. Zone I corresponds to high-temperature thermal vapourization which produces homogeneous deposition of titanium dicarbide. Zone II corresponds to real ablation whilst zone III to the spallation region which yields spall-rich deposition of TiC on samples near the target (5–8 mm) or a flat TiC deposition at longer distances (60 mm).

films deposited in these conditions are determined to be stoichiometrically TiC, as analysed by XPS. The coatings are shown to be compact layered structures which are very hard [10]. The gas phase and film compositions do not change in zone III and the only difference is the presence of a large quantity of target fragments on the film surface. It is evident that in zones II and III a non thermal equilibrium mechanism is in operation, probably related to a very rapid increase in the local temperature up to the critical temperature of the material, leading to phase explosion. The mechanism of phase explosion, proposed for laser ablation by Kelly [27,28], refers to an abrupt release of material near the thermodynamic critical temperature, due to homogeneous nucleation within a molten layer of material. Zone III, named the spallation region, which is of little interest to most industrial coaters due to its highly irregular surface deposition, is extremely interesting for biotechnological applications.

For the various power settings, titanium exposed to the plume obtained with the laser beam at a fluence of 10 J/cm² gave the most satisfactory results, with exposure time of 1 h. As depicted in Fig. 3, the surfaces obtained at varying distances from the target were topographically different. Morphology of the surface was considered optimal when the number of spalls inserted in the amorphous TiC layer was high, as shown by the SEM image at the target distance of 5 mm reported in panel A and the expression of ALP by the ROS.MER#14 cell reached the highest values. However, the distribution of the spalls at a distance of 5 mm was not homogeneous over the whole sample surface.

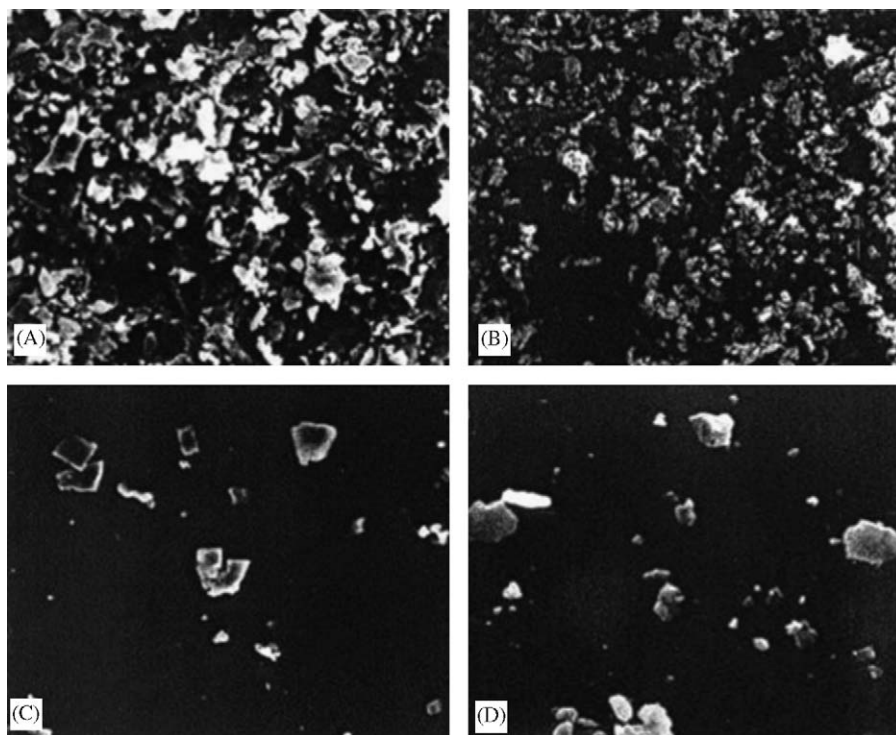


Fig. 3. SEM images (at $\times 2\text{K}$) of titanium coated with TiC at a laser fluence of 10 J/cm², 20 °C and at the following distances from the target: A = 5 mm; B = 8 mm; C = 10 mm; D = 15 mm. Smaller distances from the target result in higher spall content.

Homogeneity was obtained at a distance of 8 mm, although the surface appeared less irregular (Fig. 3B). Deposition at increasing temperature (up to 600 °C) did not alter the homogeneity but influenced only the strength with which the TiC layer was bound to the titanium substrate. At 600 °C, the deposited surface had a hardness of 3 GPa whereas that deposited at 20 °C measured 10 GPa. This latter was considered sufficient for our purpose and simpler to obtain. Deposition by PLD was therefore performed at a laser fluence of 10 J/cm², at a distance of 8 mm from the target and at a temperature of 20 °C for 1 hr. In these conditions thickness of the TiC layer was observed to be 2–3 μm. Deposition by PLD at a distance of 60 mm from the target resulted in a flat TiC surface without spalls, i.e. uniformly deposited, as observed by SEM but with a chemistry similar to that reported in Table 3 for PLD (data not reported).

3.2. XPS analysis

XPS tests (Table 3) demonstrated that in the layer deposited by PLD in the optimized conditions reported above, titanium was bound to carbon as TiC (with a stoichiometry Ti/C of approximately 1:1) for 18.6–21.5%, and to oxygen for 78.5–81.4%. Furthermore, oxygen was distributed among various titanium oxides: 11.1–13.0% as Ti₂O₃, 50.8–55.8% as TiO₂ and 14.5–14.7% as TiO. In samples deposited in the same conditions of fluence but at a distance of 60 mm the chemistry of the layer was similar (data not reported). Also very similar was the chemical composition of the TiC layer deposited with MS technology. For the optimized conditions, when TiC deposited by PLD was present at 10%, TiO₂ was found at a concentration of over 60%.

Table 3

X-ray photoelectron spectroscopy (XPS) analyses of TiC deposited with pulsed laser deposition (PLD) and magnetron sputtering (MS) technologies: chemical composition expressed as percentage

Process	TiC	TiO _n	Ti ₂ O ₃	TiO ₂	TiO
PLD	20.1 ± 1.5	80.0 ± 1.5	12.1 ± 1.0	53.3 ± 2.5	14.6 ± 0.1
MS	19.1 ± 0.1	79.4 ± 1.6	10.2 ± 0.3	52.0 ± 1.0	17.2 ± 0.3

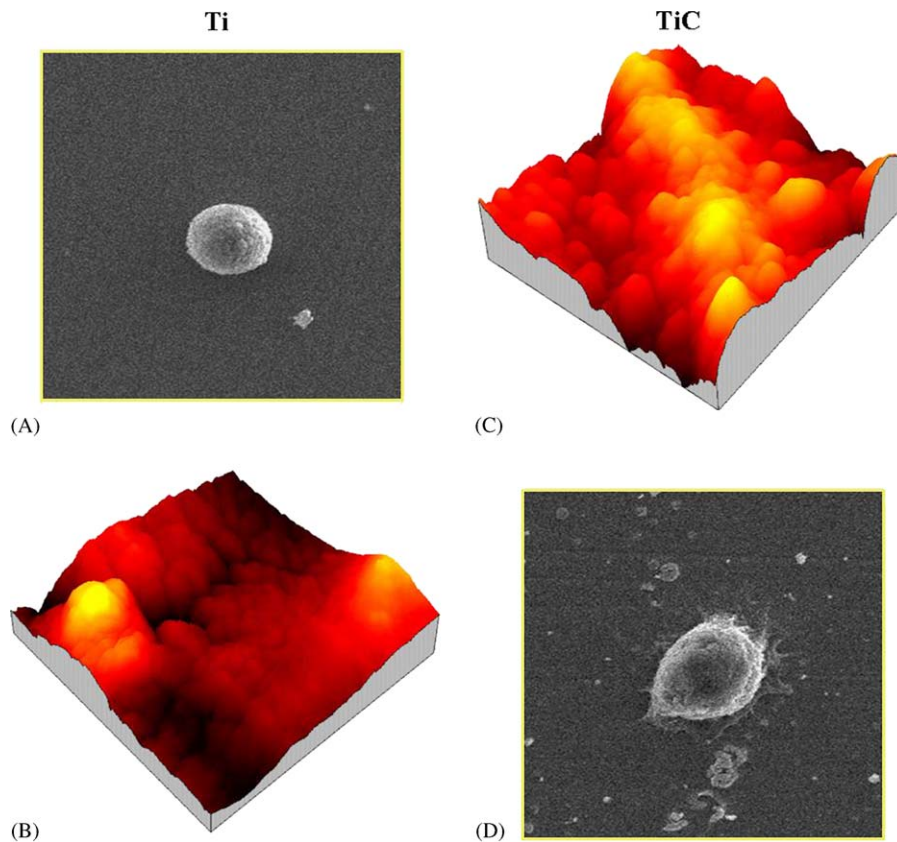


Fig. 4. Osteoblast morphology observed by scanning electron microscopy (A, D) ($\times 2$ K, 15 kV) and atomic force microscopy (B, C) after culture on uncoated (A, B) and TiC-coated (C, D) titanium samples.

3.3. Effect of TiC on osteoblast homeostasis

After 6 h of incubation on test substrates, ROS-MER#14 cells plated on TiC (Fig. 4D) were consistently firmly

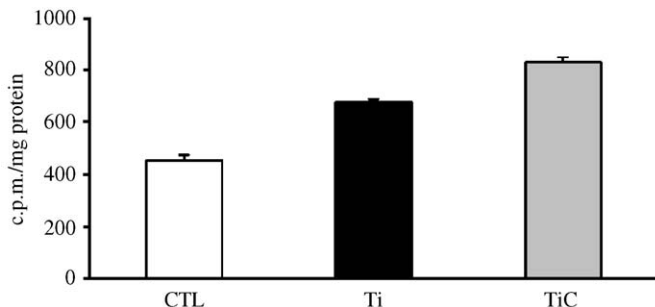


Fig. 5. ³H-thymidine incorporation (count/min/mg protein) in osteoblasts cultured on tissue culture polystyrene (CTL), uncoated (Ti) and TiC-coated titanium disks sandblasted with 60 μm zirconia particles. Results were expressed as mean ± S.E. and were representative of two independent experiments performed in triplicate.

spread through many pseudopodia compared to the cells plated on Ti (Fig. 4A), suggesting that TiC may improve osteoblastic cell spreading. AFM images confirmed that the same response over 24 h, with cells cultured on TiC-coated disks (Fig. 4C) having developed a greater number of pseudopodia compared with cells cultured on titanium disks (Fig. 4B). Cell proliferation measured by ³H-thymidine uptake was significantly greater in osteoblasts plated on titanium-based substrates compared to tissue culture polystyrene (CTL), uptake on TiC being 1.8-fold greater, and 1.5-fold on Ti (Fig. 5). Results are expressed as mean ± S.E. and were representative of two independent experiments performed in triplicate.

Genes coding for proteins involved in bone turnover: ALP, COLL-1A2, OC, BMP-4 and TGFβ were up-regulated in all cell lines (ROS.SMER #14, FOB 1.19 and hOB) grown on titanium disks sandblasted with 60 μm zirconia particles and coated with TiC deposited by PLD compared to uncoated Ti disks when measured by semiquantitative PCR (Figs. 6A–C). This observation,

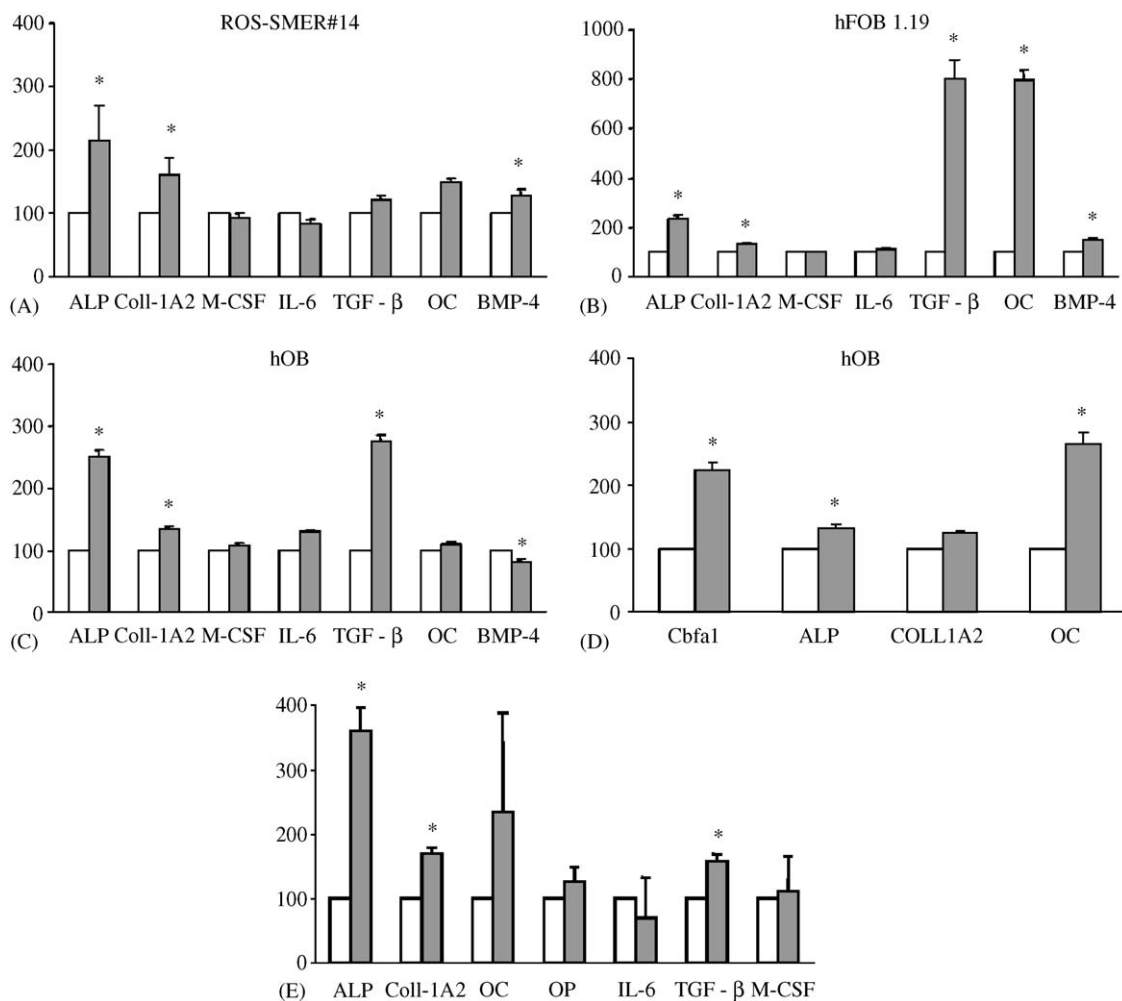


Fig. 6. Gene expression of different osteoblast cells by semiquantitative RT-PCR analysis (A, B, C) and real time RT-PCR (D) after culture on Ti (white bar) and TiC-coated (black bar) titanium disks sandblasted with 60 μm zirconia particles. In panel E the biological response of ROS.MER#14 cells grown on Ti disks sandblasted with 60 μm zirconia particles (white bar) and TiC coated by the MS technology (grey bar) are reported. Signals were quantified by densitometric analyses and values were normalized for GAPDH and expressed as per cent of Ti. Data are presented as mean ± S.E. of at least three independent experiments. Differences were analysed by one-way analysis of variance, with $p < 0.05$ being considered statistically significant (*).

including upregulation of *Cbfa1/ostf2*, was confirmed by Q-RT-PCR in hOB (Fig. 6D). Additionally, osteoblast-contribution to osteoclastogenesis and osteoclast activity, via cell–cell interaction and paracrine stimulation, was not significantly altered after culture on TiC compared to Ti, as determined by the measurement of IL-6 and M-CSF expression. In Fig. 6E, the biological response of ROS.MER#14 cells grown on Ti disks sandblasted with 60 μm zirconia particles are reported, together with TiC coated by the MS technology. In this case, two genes involved in bone turnover are up-regulated similarly to the results reported in panel A (ROS.MER#14 cells on TiC coated by PLD). Signals were quantified by densitometric analyses and values were normalized for GAPDH. Data are presented as mean \pm S.E. of at least three independent experiments. Differences were analysed by one-way analysis of variance, with $p < 0.05$ being considered statistically significant.

3.4. Effects of substrate topology on osteoblast gene expression

To determine if the effects of PLD on gene expression were due to surface topography rather than chemistry, and to investigate synergy between them, PLD deposition was performed on titanium samples whose surface was mirror polished (mp), blasted with 60, 120 and 150 μm zirconia particles. As shown in Fig. 7 (data normalized against uncoated Ti disks), the roughness of the substrate influenced the stimulation in ROS.MER#14 cells of the ALP, COLL-1A2 and OC genes, the largest effect being upregulation of all genes by TiC, except after blasting with 150 μm zirconia particles, which resulted in a downregulation on TiC compared with Ti.

To interpret the influence of spallation due to PLD on gene upregulation, increase of the sample distance from the

target (from 8 to 60 mm) to produce a flat, uniform coating was analysed through the modulation of ALP, the most responsive gene. Results (Table 4), when normalized against mirror-polished Ti, demonstrate that roughness induced by cutting or blasting with 60 and 120 μm zirconia particles upregulated ALP by 50% for Ti (lines 4, 7 and 9). A flat TiC coating, generated at a distance of 60 mm, gives a further upregulation of ALP (lines 3 and 6) demonstrating that a TiC layer without spalls is also beneficial to the upregulation of ALP. Microroughness due to coating within the spallation region at the optimized distance of 8 mm (lines 2, 5, 8 and 10) caused the greatest upregulation of ALP. Only treatment with 150 μm zirconia particles (lines 11 and 12) had a negative effect on ALP upregulation.

3.5. In vivo experiments

After 4 weeks of implantation of dental implants in the femurs of rabbits, bone density around the implants, evaluated by X-ray mammography, demonstrated an increase in bone density around the TiC coated implants compared to untreated Ti (Fig. 8B) and to an implant inserted at time zero (Fig. 8A). After 8 weeks the bone density around the implant was increased around both the uncoated and coated implants (Fig. 8C) but this appears to be greater in the latter. Thin slices of the bone–implant interface clearly demonstrated increased bone growth macroscopically (Fig. 8D). The thin slices exposed overnight to X-ray micro radiography (24) gave the pictures reported in panel E of Fig. 8: around the coated implants a major bone density was detectable.

The same osseointegration response was observed in histological sections by light microscope in sheep. As shown in Fig. 9A, space between the implant (the black

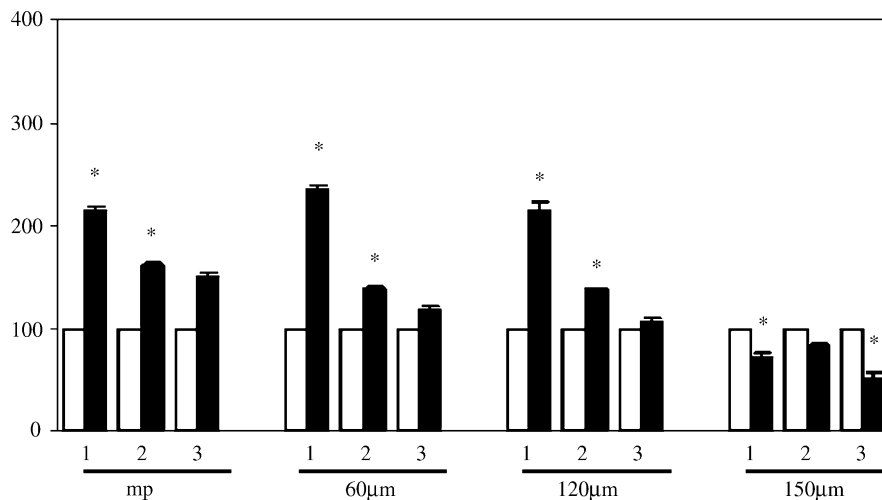


Fig. 7. Dependency of surface roughness on the modulation of (1) ALP; (2) COLL-1A2 and (3) OC genes. ROS-SMER#14 cells were cultured on mirror polished titanium (mp) and titanium disks sandblasted with 60, 120 and 150 μm zirconia particles (black bars). Semiquantitative RT-PCR were performed and signals were quantified by densitometric analysis. Values were normalized for GAPDH and expressed as per cent of uncoated titanium (white bars). Data are presented as mean \pm S.E. of at least three independent experiments. Differences were analysed by one-way analysis of variance, with $p < 0.05$ being considered statistically significant (*).

Table 4
Effects of substrate topology on osteoblast gene expression^a

	Sample	ALP	COLL-1A2
1	Ti mp	100	100
2	TiC mp 8 mm	266	139
3	TiC mp 60 mm	191	136
4	Ti N	150	91
5	TiC N 8 mm	224	108
6	TiC N 60 mm	211	71
7	Ti S 60	150	80
8	TiC S 60 8 mm	234	139
9	Ti S 120	150	75
10	TiC S 120 8 mm	214	137
11	Ti S 150	60	70
12	TiC S 150 8 mm	70	83

mp: titanium mirror polished.

N: rough cut titanium, not sandblasted.

S60: sandblasted with 60 μm zirconia particles.

S120: sandblasted with 120 μm zirconia particles.

S150 sandblasted with 150 μm zirconia particles.

^aDensitometric values of electrophoretic band areas of PCR products normalized to mirrored Ti.

part in each panel) and existing bone, containing some bone fragments derived from the surgical procedure, is clearly visible in this section taken from an implant inserted at zero time. After 2 weeks, this space contained new formed spongy bone tissue around the uncoated Ti implants (Fig. 9B) with few cells in the marrow spaces. In the case of the TiC-coated implants, the space around the implant after 2 weeks was filled by spongy new formed bone with very cellular and vascularized bone marrow (Fig. 9C); at four weeks a clear maturation towards a cortical bone is observed (Fig. 9D).

Additional experiments in the rabbits to investigate the rate of bone formation demonstrated rapid onset of bone formation in TiC around the implanted rods compared to Ti (Fig. 10). Significant bone was observed to have accumulated at the implant–bone interface, shown as red staining, at the two week time period in TiC and especially within the cancellous zone. Significant quantities of new bone were also formed within the cortical zone at 1 week in TiC (panel B). Conversely, only a small amount of bone had formed around the Ti implants at 2 weeks and no visible bone formation at 1 week. Significant new bone can be seen in both implant types on the opposite side of the bone to implantation due to bone remodelling caused by loss of bone strength due to drilling.

4. Discussion

The results presented in this study demonstrate that a layer of TiC covering titanium have beneficial effects on bone forming cells both in vitro and in vivo. These effects are due to many factors involving both the morphology of the TiC layer and its surface chemistry. A homogeneous layer of TiC, obtained with PLD technology increased the

upregulation of genes required for bone formation in multiple cell lines compared to expression obtained with untreated titanium, but the layer produced with by PLD combined with microroughness demonstrated the greatest stimulating effect on osteoblasts.

It is widely reported that surface roughness has a profound effect on osteoblast attachment, proliferation and differentiation [1,29–38]. The precise stimulating effect on osteoblasts by the PLD-deposited TiC layer is related to two principle factors: one mechanical and one chemical as evidenced also by other authors [1,30,35–36,38]. The layer of TiC obtained in the spallation region is characterized by the presence of many spalls which provides microroughness representing the mechanical factor. The importance of this topographical factor can be understood from an assessment of ALP expression of osteoblasts on deposition layers of the same composition but with varying morphology: rough cutting or sandblasting with 60 or 120 μm zirconia particles provides no difference among the group, all these treatments causing approximately 50% more stimulation than that elicited by the mirror polished titanium samples. On the other hand, macroroughness, for example in the case of blasting with 150 μm particles, does not appear to provide a stimulatory effect, and in this case a slight inhibition because this treatment imposed so large a modification to the titanium surface as to induce a less suitable attachment of the osteoblast cell. However, TiC deposition without spallation delivered increased expression approximately between 40% and 90% for cut and polished samples, indicating both that the surface chemistry is influencing apparent osseointegration, and that roughness and chemistry are acting in an additive fashion, suggesting two separate mechanisms are indeed responsible for the upregulation of the genes required for neo bone formation. In our experiments, maximal stimulatory effect

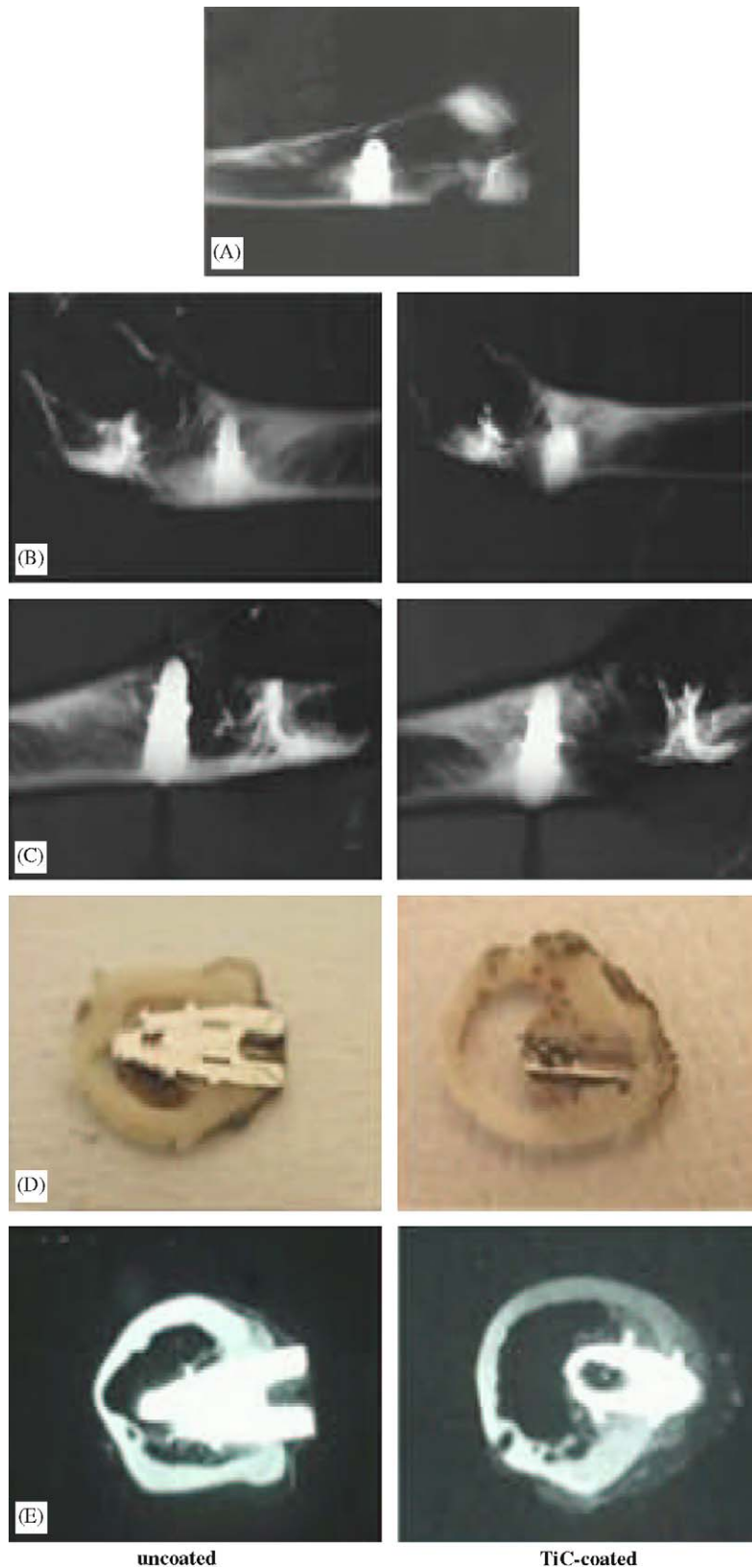


Fig. 8. X-ray analysis of implants in rabbits. At zero time (A), after four (B) and eight (C) weeks implantation animals were sacrificed and bone density around the implants was evaluated by X-ray mammography. Radiographs and pictures at the left are related to uncoated implants, those at the right to the TiC-coated implants which show a major bone density around the implants. The 8-week bones containing the implants were excised and cut in slices of approx 60 μm . Images of slices (D) were taken and then exposed overnight to a low intensity X-ray microradiograph (E). Bone density around the TiC-coated implant was higher than in uncoated Ti implant.

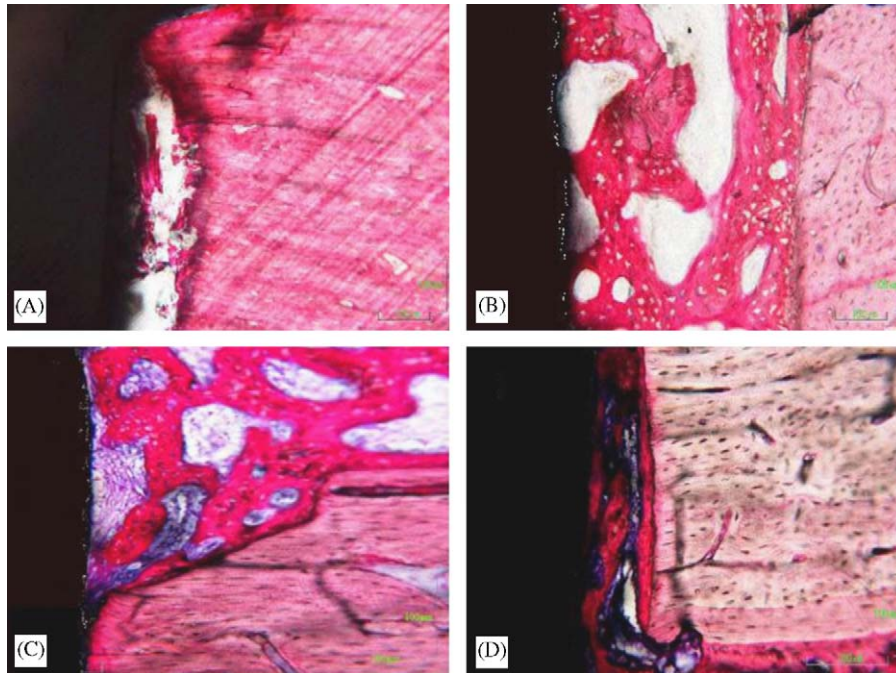


Fig. 9. Histology of uncoated titanium dental implants in sheep at zero time (A), after 2 weeks (B) and TiC-coated implants after 2 weeks (C) and 4 weeks (D). At zero time (panel A), some bone fragments derived from the surgical procedure can be observed in the space between the implant (black part) and the bone. After 2 weeks, this space contained newly formed spongy bone tissue around the uncoated Ti implants (Fig. 9B) with few cells in the marrow spaces. In the case of the TiC-coated implants, the space around the implant after 2 weeks was filled by spongy new formed bone with very cellular and vascularized bone marrow (Fig. 9C); at 4 weeks a clear maturation towards cortical bone is observed (Fig. 9D).

was achieved when TiC was deposited with homogenous spallation. It should also be recognized that the stimulation caused by TiC on osteoblast cell activity appears to be highly physiological since the genes stimulated by TiC are mainly involved in cell differentiation.

XPS analyses have demonstrated that in the layer deposited by PLD, only about 20% of titanium is bound to carbon, as TiC (with a stoichiometry Ti/C of about 1:1), and approximately 80% is bound to oxygen. Furthermore, oxygen is distributed among various titanium oxides: about 12% as Ti_2O_3 , 53% as TiO_2 and 14.5% as TiO. From assessment of different carbides created prior to optimization of the PLD process, beneficial stimulation of osteoblast activity only occurred when all three oxides were present in these approximate concentrations. In particular, bone formation gene upregulation only occurred when Ti_2O_3 was present at 10–13%, TiO_2 at 50–57%, TiO at 14–18% with TiC occurring at 18–22%. In all TiC coatings where TiO_2 comprised over 60% coupled with TiC present at 10%, no stimulatory effect on osteoblasts was observed. Furthermore, these results suggested that amongst all the oxides, the presence of Ti_2O_3 at 10–13% was of paramount importance. The effect of surface chemistry in the absence of topographical effects was confirmed by observing the osteoblast stimulation due to culture with films produced by MS PVD, a deposition technique which produces TiC without spallation. XPS analysis confirmed very similar chemistry (Table 3) with similar biological effects (Fig. 6E).

In vivo results, in two different animals, strongly demonstrate enhanced bone formation over a 4–8-week time frame. However, in applications such as dental and orthopaedic implants, where early loading is beneficial to the rehabilitation of the patient, the rate of early bone formation is critically important. By continuous monitoring using intravital dyes, it was possible to detect significant bone formation occurring within the first week around the whole of the implant interface in TiC-coated implants, where only a small degree of neo bone formation was observed in uncoated Ti suggesting that the TiC was driving early osseointegration compared to untreated titanium implants. The degree of enhancement would appear to be many times greater, from these observations, than the indications from in vitro investigations. Furthermore, the in vivo models validate the use of expression of bone-forming genes as an indicator of bone-contacting biomaterial performance, in particular *Cbfa1/osf2*, ALP, COLL-1A2, OC, BMP4 and TGF β .

5. Conclusions

In conclusion, taken together these results strongly suggest that the use of TiC as a coating on orthopaedic and dental prostheses would improve the osseointegration process in humans, stimulating osteoblast proliferation, adhesion and activity. In addition to protecting the titanium from the aggressive attacks of biological fluids and tissues and increasing implant hardness, it is concluded

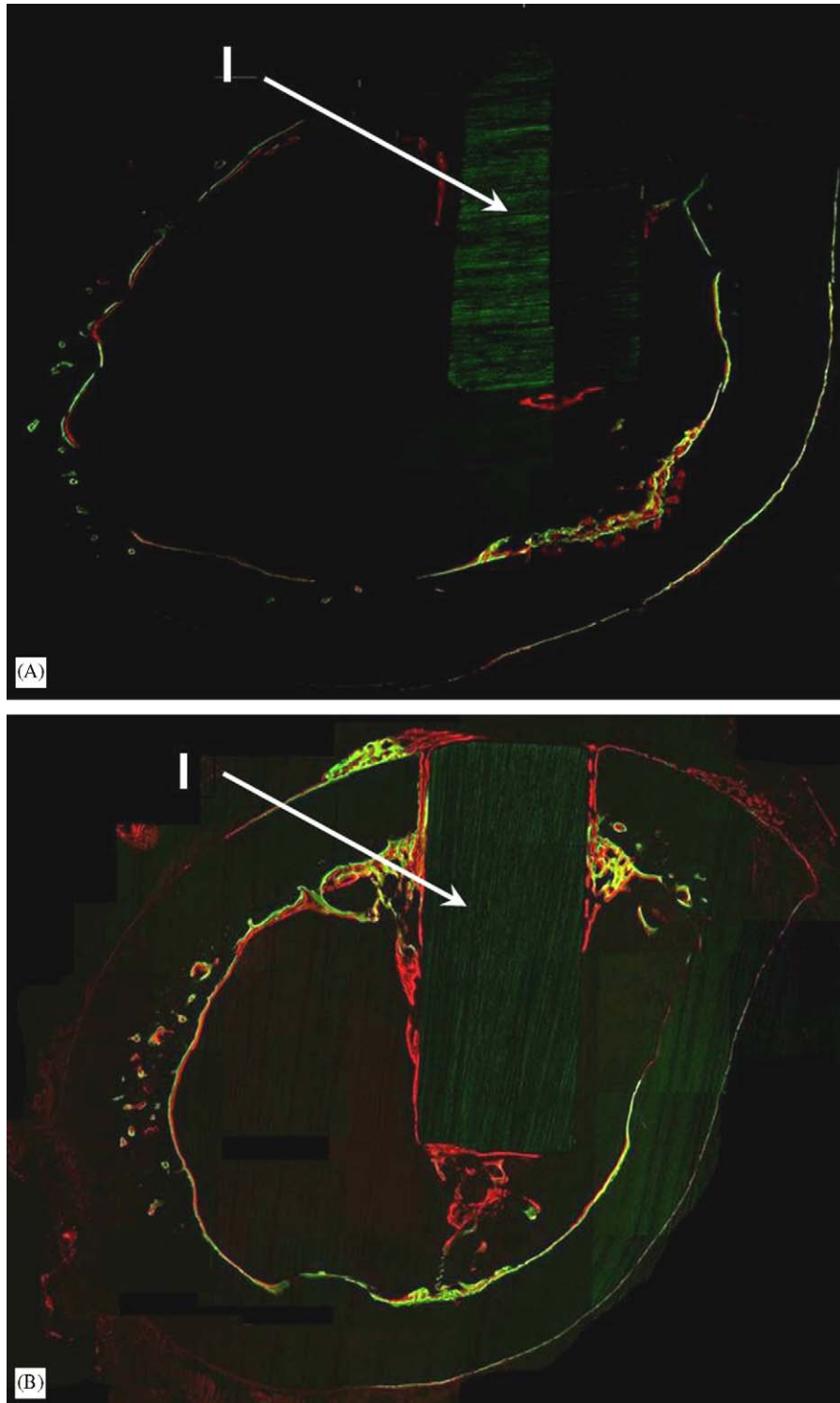


Fig. 10. Confocal microscopy of intravitaly stained implants in rabbits: (A) uncoated Ti; (B) TiC-coated Ti. “I” indicates location of implant. Stains indicate bone formation at 1 week (green), 2 weeks (red) and 5 weeks (yellow). Bone formation at 6 weeks (orange) or 8 weeks (blue) is not visible in these images.

that coating titanium implants with a layer of TiC achieves these further goals:

- (a) increases the biocompatibility of titanium;
- (b) stimulates proliferation, adhesion and differentiation of osteoblasts.

Acknowledgements

We would like to thank C. Coluzza and N. Caretto for the AFM images, S.M. Barinov for useful discussion, R. Aimo for preparing samples treated by MS, and A. Ruggero and D. Martini for performing sample

histology. The technical assistance of P. Villani, G. Rau and M. Moriggi is gratefully acknowledged. Funding was received from the European Commission under the Industrial & Materials Technologies Growth Programme of the Fifth Framework. We would also like to acknowledge the EPSRC for provision of an Advanced Research Fellowship for Nicholas Rhodes. Parts of the research were performed as part of the Interdisciplinary Research Collaboration in Tissue Engineering for which funds were provided by the BBSRC, MRC and EPSRC.

References

- [1] Kurella A, Dahotre NB. Review paper: surface modification for bioimplants: the role of laser surface engineering. *J Biomater Appl* 2005;20:5–50.
- [2] Pourbaix M. Atlas of electrochemical equilibria in aqueous solutions. New York: Pergamon Press; 1966.
- [3] Black J. Biological performance of biomaterials. Fundamentals of biocompatibility. 2nd ed. New York: Marcel Dekker Inc.; 1993.
- [4] Park JB, Lakes RS. Biomaterials—an introduction. New York: Plenum Press; 1992.
- [5] Nalwa HS. Handbook of thin film materials. Deposition and processing of thin films, vol. 1. San Diego: Academic Press; 2002.
- [6] Miller JC, Haglund RF. Laser ablation and desorption. San Diego: Academic Press; 1998.
- [7] Teghil R, D'Alessio L, Zaccagnino D, Ferro D, Marotta V, De Maria G. TiC and TaC deposition by pulsed laser ablation: a comparative approach. *Appl Surf Sci* 2001;173:233–41.
- [8] Willmott PR, Huber JR. Pulsed laser vaporization and deposition. *Rev Modern Phys* 2000;72:315–28.
- [9] Horwitz JS, Sprague JA. Film nucleation and film growth in pulsed laser deposition of ceramics. In: Chrisey DB, Hubler GK, editors. Pulsed laser deposition of thin films. New York: Wiley; 1994. p. 229.
- [10] De Maria G, Ferro D, D'Alessio LD, Teghil R, Barinov SM. Hardness of titanium carbide films deposited on silicon by pulsed laser ablation. *J Mater Sci* 2001;36:929–35.
- [11] Barinov SM, Ferro D, Bartuli C, D'Alessio LD. Hardness of hafnium carbide films deposited on silicon by pulsed laser ablation. *J Mater Sci Lett* 2001;20:1485–7.
- [12] Migliaccio S, Davis VL, Gibson MK, Gray TK, Korach KS. Estrogens modulate the responsiveness of osteoblast-like cells (ROS 17/2.8) stably transfected with estrogen receptor. *Endocrinology* 1992;130:2617–24.
- [13] Hunt JA, Callaghan JT, Sutcliffe CJ, Morgan RH, Halford B, Black RA. The design and production of Co–Cr alloy implants with controlled surface topography by CAD–CAM method and their effects on osseointegration. *Biomaterials* 2005;26:5890–7.
- [14] Teghil R, Guidoni AG, Mele A, Piccirillo S, Coreno M, Marotta V, et al. Pulsed laser induced ablation applied to epitaxial-growth of semiconductor materials: selenides and tellurides plume analysis. *Surf Interface Anal* 1994;22:181–5.
- [15] Ferro D, Scandurra R, Latini A, Rau JV, Barinov SM. Hardness of electron beam deposited titanium carbide films on titanium substrate. *J Mater Sci* 2004;39:329–30.
- [16] Castle JE, Salvi AM. Chemical state information from the near-peak region of the X-ray photoelectron background. *J Electron Spectrosc Relat Phenom* 2001;114:1103–13.
- [17] Briggs D, Seah MP. Practical surface analysis by Auger and X-ray photoelectron spectroscopy. New York: Wiley; 1983.
- [18] Owen TA, Aronow M, Shalhoub V, Barone LM, Wilming L, Tassinari MS, et al. Progressive development of the rat osteoblast phenotype in vitro: reciprocal relationships in expression of genes associated with osteoblast proliferation and differentiation during formation of the bone extracellular matrix. *J Cell Physiol* 1990;143:420–30.
- [19] Aubin JE. Advances in the osteoblast lineage. *Biochem Cell Biol* 1998;76:899–910.
- [20] Sodek J, Zhang Q, Goldberg HA, Domenicucci C, Kasugai S, Wrana JL, et al. Non-collagenous bone proteins and their role in substrate-induced bioactivity. In: Davies JE, editor. The bone–biomaterial interface. Toronto: University of Toronto Press; 1991. p. 97–110.
- [21] Sodek J, Cheifitz S. Molecular regulation of osteogenesis. In: Davies JE, editor. Bone engineering. Toronto: EM Squared Inc.; 2000. p. 31–43.
- [22] Livak KJ, Schmittgen TD. Analysis of relative gene expression data using real-time quantitative PCR and the 2(T)(-Delta Delta C) method. *Methods* 2001;25:402–8.
- [23] Pfaffl MW. A new mathematical model for relative quantification in real-time RT-PCR. *Nucl Acids Res* 2001;29:2002–7.
- [24] Engström A. Autoradiography. In: Oster G, Pollister AW, editors. Physical techniques in biological research, vol. 3. New York: Academic Press; 1958. p. 489–544.
- [25] D'Alessio L, Salvi AM, Teghil R, Marotta V, Santagata B, Brunetti B, et al. Silicon supported TiC films produced by pulsed laser ablation. *Appl Surf Sci* 1998;134:53–62.
- [26] D'Alessio L, Galasso A, Santagata A, Teghil R, Villani AR, Villani P, et al. Plume dynamics in TiC laser ablation. *Appl Surf Sci* 2003;208:113–8.
- [27] Kelly R, Miotello A. Contribution of vaporization and boiling to thermal-spike sputtering by ions or laser pulses. *Phys Rev E* 1999;60:2616–25.
- [28] Kelly R, Miotello A. Does normal boiling exist due to laser-pulse or ion bombardment? *J Appl Phys* 2000;87:3177–9.
- [29] Puleo DA, Holleran LA, Doremus RH, Bizios R. Osteoblast responses to orthopedic implant materials in vitro. *J Biomed Mater Res* 1991;25:711–23.
- [30] Lincks J, Boyan BD, Blanchard CR, Lohmann CH, Liu Y, Cochran DL, et al. Response of MG 63 osteoblast-like cells to titanium and titanium alloy is dependent on surface roughness and composition. *Biomaterials* 1998;19:2219–32.
- [31] Boyan BD, Schwartz Z. Modulation of osteogenesis via implant surface design. In: Davies JE, editor. Bone engineering. Toronto: EM Squared Inc.; 2000. p. 232–9.
- [32] Keller JC, Schneider GB, Stanford CM, Kellogg B. Effects of implant microtopography on osteoblast cell attachment. *Implant Dent* 2003;12:175–81.
- [33] Ronold HJ. Analysing the optimal value for titanium implant roughness in bone attachment using a tensile test. *Biomaterials* 2003;24:4559–64.
- [34] Martin JY, Schwartz Z, Hummert TW, Schraub DM, Simpson J, Lankford J, et al. Effect of titanium surface roughness on proliferation, differentiation and protein synthesis of human osteoblast-like cells (MG63). *J Biomed Mater Res* 1995;29:389–401.
- [35] Suzuki K, Aoki K, Ohya K. Effects of surface roughness of titanium implants on bone remodelling activity of femur in rabbits. *Bone* 1997;21:507–14.
- [36] Anselme K, Bigerelle M. Topography effects of pure titanium substrates on human osteoblast long-term adhesion. *Acta Biomater* 2005;1:211–22.
- [37] Schwartz Z, Nasatzky E, Boyan BD. Surface microtopography regulates osteointegration: the role of implant surface microtopography in osteointegration. *Alpha Omegan* 2005;98:9–19.
- [38] Anselme K, Bigerelle M. Statistical demonstration of the relative effect of surface chemistry and roughness on human osteoblast short adhesion. *J Mater Sci: Mater Med* 2006;17:471–9.